LH LepR neurons directly drive sustained food seeking behavior after AgRP neuronal deactivation via neuromodulation of NPY.

1. Abstract

Agouti-related protein (AgRP) has been believed to be the main driver of feeding behaviors ever since its discovery. However, recent studies using fiber photometry and optogenetics proved that feeding behaviors are not directly driven by AgRP neurons (temporal discrepancy between neuronal activity and behavior). To resolve this paradox, we conducted novel multi-phase feeding experiments to scrutinize the dynamics of AgRP. Fiber photometry study showed that AgRP neurons start to deactivate even before the initiation of the food search phase. Using optogenetics, we could prove that the feeding behavior induced by AgRP neuron activation had substantial temporal delay and the feeding behavior was sustained for substantial time even after cessation of optogenetic activation. These results indicate that AgRP neurons are not the direct driver of feeding behavior and another downstream neuron is the driver of feeding behavior. Leptin receptor (LepR) neurons in the lateral hypothalamus (LH). LH LepR neurons were activated before voluntary food search behavior initiation and showed robust increase after food approach behavior. Artificial activation of LH LepR neurons drives food search and food approach behavior. In accordance, chemogenetic activation of LepR neurons increased food search and food approach behaviors. Lastly, slice calcium imaging results showed the possibility that NPY from the AgRP neurons could be the downstream neuromodulator of AgRP neuron, driving LH LepR neuron activation. Overall, our study shows that AgRP neurons are not the direct drivers of feeding behavior, whereas LH LepR neurons directly drive sustained food seeking behavior.

2. Introduction

Feeding is a food directed behavior that has a series of temporal sequences [1, 2]. To compensate homeostatic needs and seek rewards, our body performs consecutive food related behavior. We have previously suggested the concept of multi-phase feeding behavior [3]. The initiation of feeding behavior requires cumulation of motivation for a desired outcome (Phase 1: Craving Phase). When accumulation of motivation reaches a certain behavioral threshold, goal-driven exploring behavior is initiated (Moment 1; Behavior Onset Moment). After behavior initiation, a locomotive searching behavior for undiscovered food is sustained (Phase 2: Search Phase) until the food is discovered (Moment 2: Discovery Moment). After food discovery, a locomotive approaching behavior toward the discovered food is sustained (Phase 3: Approach Phase) until food contact (Moment 3: Contact Moment). After food contact, consummatory behavior is sustained (Phase 4: Consumption Phase) until the termination of consumption (Moment 4: Consumption Termination Moment) (Fig 1).

Regarding feeding behavior, AgRP neurons in the arcuate nucleus (ARC) of the hypothalamus have been believed to be the main driver of feeding behavior. AgRP neurons have been believed to be activated during energy deprivation and to be deactivated after energy consumption [4-6]. However recent studies using real-time calcium signals have shown that AgRP neurons are rapidly deactivated on presentation of food, which is even before the consumption of food [7-9]. However, these studies could not distinguish which of the four phases of feeding behavior is responsible for the AgRP neuron deactivation, since the food presentation procedure included mixture of multiple cognitive and behavior components (food discovery and food approach). Contrary to the deactivating results of real time observation of AgRP neurons during feeding behavior, artificial activation of AgRP neurons induced feeding behavior but were not capable of rapidly inducing feeding behavior [10] and had sustained effects on feeding after artificial deactivation [11]. Indeed, results on feeding behavior of AgRP neurons during real time observation and artificial simulation are paradoxical. Thus, multi-phase feeding is an essential theory and strategy to put distinction to the ambiguous neuronal mechanism of AgRP neurons. If the AgRP neurons do not lead feeding behavior after the craving phase, then other neurons downstream to the AgRP neurons should be the main neuron directly driving feeding behavior [10, 12, 13].

Recent studies suggest NPY neuromodulation as necessities for sustained feeding behavior after AgRP neuron deactivation [11]. However, it is unclear which brain area receives NPY signals to activate the downstream neurons. Brain areas that receive AgRP neuronal inputs are known to be parabrachial nucleus, lateral hypothalamus, and the paraventricular nucleus [8, 10]).

Among these regions, the lateral hypothalamus (LH) has been studied in various aspects related to feeding behavior and has been regarded as a feeding center [14-24]. Subpopulation circuits in the LH were reported to show immediate response to feeding [14, 16, 17]. LH GABA and glutamate neurons were reported to regulate hunting and evasion [25]. Among the GABA neuron population, leptin receptor neurons (LepR) in the LH have been suggested to be involved in feeding [26-28]. However, the role of LH LepR neurons on feeding behavior have not been fully investigated in a multi-phase manner.

To investigate the role of AgRP and the LepR neurons in multi-phase feeding behavior, we conducted novel behavioral experiments that could distinguish feeding behavior into separate phases. Fiber photometry was used as tools to discover that AgRP neurons naturally deactivated even before initiation of the search phase. This result is in consistent with recent studies suggesting future prediction of AgRP neurons [29]. Our optogenetic results on AgRP neurons show delayed feeding behavior on AgRP activation in fed mice. Sustained feeding behavior could also be shown after artificial deactivation of AgRP neurons Our novel real-time calcium signal results on LH LepR neurons during feeding behavior show that they drive feeding behavior. LepR neuronal activity initiate from the search phase, incline during the approach phase, rapidly increase at food contact and sustain during consumption. Chemogenetic activation of LepR neurons were able to evoke the search phase and approach phase in fed mice. NPY neuromodulation increased LH LepR neuron activity in brain slice calcium imaging studies. This suggests the possibility of interaction of AgRP and LepR neurons during feeding behavior.

3. Result

ARC Neurons Show Distinct Temporal Dynamics of Feeding Behavior

In order to identify the exact role of AgRP neurons during food seeking behavior, we first conducted a series of behavioral experiments that could split the sequential behaviors of food seeking behavior during fiber photometry recordings with mice expressing GCamp6s in AgRP neurons (Fig 2 A, B). First, to have an integrated overview of the series of experiments, fasted mice were tested in a scheduled timing multi-phase test in a specialized chamber (Trials 90, n=6). Mice were let to freely initiate food seeking behavior after manual trial initiation. As a result, we could observe AgRP neuron activity decreasing even before trial initiation (Fig 2 D). This consists with reports that AgRP signal changes could be resulted from future prediction of the homeostatic change [29]. Quantification of average AgRP deactivation in all the trials indicated that AgRP deactivation mostly happened before food discovery (Fig 2 C,D). Furthermore, we could observe that POMC neurons started to increase at visual food discovery, but its overall increment happened during food consumption. Quantification of POMC neuronal activation also showed mean POMC neuronal activity to increase during food consumption (Fig 2 D). These findings indicate that further phase specific investigation is necessary to rigorously determine the function and dynamics of AgRP and POMC neurons.

To scrutinize the most fluorescence change of neuronal activity in the multiphase behavior of the LLC test, we next performed a voluntary timing search test to identify the temporal dynamics at the initiation of search phase (Fig 2 F). As a result, we could observe that AgRP neuronal activity started to decrease even before the behavioral onset (Fig 2 G, H, I). To quantify the correlation between neuronal onset and behavioral onset, we defined neuronal onset with 3rd derivatives of AgRP signals. [30, 31](Fig 2 J). Timing of neuronal onset happened approximately 7s before behavioral onset. This suggests that AgRP neuronal activity changes during the craving phase before the behavioral initiation of the search phase. We then investigated AgRP neuronal change during a devised vertical approach test (Fig 2 M). Mouse were let to spontaneously approach food in position that was either obtainable or unobtainable in rearing position (Fig 2 M). AgRP neural activity decreased during approach to both conditions. AgRP neural activity sustained below the baseline only when food was obtainable. (Fig 2 N, O, P). POMC neural activity increased on initiation of the approach phase, decreased when food was unobtainable and increased during food consumption (Fig 2 Q, R, S). These results are rigorous evidence that AgRP does not function as suggested in past studies.

Artificial Activation of AgRP Neurons Does Not Immediately Drive Feeding Behavior and Feeding Behavior is Sustained after Artificial Deactivation of AgRP

To further specify the role of AgRP in multi-phase feeding behavior we examined AgRP neurons during optogenetic stimulation. AgRP cre mice were injected with cre dependent ChR2 virus at the ARC unilaterally (Fig 3 A). Blue laser was delivered to mice in an open-field test vertical food approach test (Fig 3 C, J). Our optogenetic results matched previous reports; artificial AgRP stimulation increased food intake and approach to food in the open field test [4] [8] [7]. Distance to food decreased, and velocity, biting bouts and in zone time of mouse increased during laser stimulation. Sustaining effects could also be observed even after laser inactivation with the following analysis categories (Fig 3 E). Tracking the location of mice displayed increased duration of mouse in food zone during

laser stimulation and laser deactivation (Fig 3 D). Further analysis of the first and last minutes during stimulation and post-stimulation showed substantial latency between optogenetic activation moment to the initiation of food consumption and sustaining effects leading to feeding behavior after optic stimulation was removed (Fig 3 G, H). The latency between optogenetic stimulation and behavior initiation was 86s, and sustained effects lasted about 220s when stimulation was removed (Fig 3 F). The cumulative distribution of the probability of all mice to the distance to food showed distant location in the first minute of stimulation compared to the last minute of stimulation. Quantification after laser deactivation showed opposite results. Mice were adjacent to food during the first minute, but distant during the last minutes (Fig 3 I).

We then investigated the effect of optogenetic stimulation during the vertical approach test to verify whether artificial AgRP neuron activation increases not only food intake, but food approach (Fig 3 J). Velocity increased during optogenetic stimulation, and approach to food while staying in the food zone increased compared to non-food zone (Fig 3 L). Whole raster plot of approach bouts to food also showed increased approach to food. Consistent to the open field test, approach to food happened after minutes, and sustained even after deactivation (Fig 3 N). The mean latency to approach food after artificial activation was 60(s) and sustained for about 180(s) even after laser deactivation (Fig 3 Q). Tracking the location of mouse during the vertical approach test also showed increased duration in the food zone (Fig 3 K). Quantification of frequency and overall duration also showed substantial difference between optogenetic activation and inactivation (Fig 3 M). Overall analysis of time bins showed overall increase after the first minutes if laser stimulation while sustained effects could be observed for up to 2 minutes on laser omission (Fig 3 O) [11]. Considering the effect of optogenetic stimulation on mouse behavior and results from real-life calcium signal recordings these results do not consist with each other. If AgRP neurons were to be the direct driver of food seeking behavior, postponed food seeking behavior before optic stimulation, sustained food seeking behavior after omission of laser and decreased photometry signals during food search and approach cannot conclude that AgRP neurons drive the whole feeding behavior. Altogether, these results show that AgRP neurons have limited roles to induce feeding behavior by mainly driving the craving phase and is not required to sustain activity for behavioral onset to food. Thus, to determine specific neurons that directly influence food search, approach behavior we chose to investigate the LH, a well-studied food center known to have many neuronal circuits to the ARC

GABA neurons and LepR neurons show opposing response to Food Contact

We hypothesized that after the deactivation of AgRP neurons at food search initiation, certain population in the LH GABA would have to activate after food search initiation regarding its role in acute feeding behavior in optogenetics[32-34]. To determine if GABA neurons had any specific response during food interaction, we first compared the neural activation during food contact and non-food contact (Fig 4 B). Cre-dependent GCamp6s virus were injected into the LH GABA neurons to measure calcium signals during fiber photometry in the contact test (Fig 4 A). GABA neuron activity slightly increased on food contact and decreased on the start of food consumption phase whereas no significant change occurred with non-food interaction (Fig 4 C, D, E, I, J). To elaborately investigate the mass sub-population of GABA neurons [35], we then chose to investigate the LepR neurons considering its regulatory effect on feeding. Primarily, fiber photometry on mice expressing GCamp6s in the LH LepR (Fig 4 A) was conducted with fasted mice during the contact test

(Fig 4 B). Surprisingly, we found rapid increase of neuronal activity in the LepR neurons after food contact. These results were opposing to the results on LH GABA neurons, whereas contact with non-food had no effect on LepR activity (Fig 4 F, G, H, K, L). Initiation of LepR neuronal activity occurred even before food contact. To further specifically define the neuronal mechanism of LepR neurons in multi-phase behavior, we conducted multi-phase experiments that would help determine specific dynamics of LepR neurons during each phase of feeding behavior.

LH LepR Neurons are Activated Before Voluntary Food Search Initiation and Show Robust Increase after Food Approach

To further determine specific temporal dynamics of LepR neurons during multi-phase food seeking behavior, we investigated neural activity during the multi-phase feeding test with fiber photometry (Fig 5 A). We first examined in-vivo calcium activity of LH GABA neurons. GABA neurons were activated at initiation of the search phase, increased until discovery of food and decreased on food contact (Fig 5 B). However, LepR neuronal activity had different directional change in temporal dynamics compared to GABA neurons. Neural change occurred at initiation of the search phase and increased during the food approach phase and the food consumption phase (Fig 5 C, D). However, manually determining the trial start moment in the multi-phase test made it vague to determine which phase LepR neurons initiate activity.

In order to determine the behavior causing neural activation of LepR neurons, we trained mice in the voluntary search test to precisely observe LepR neuronal change during voluntary motivated food search initiation (Fig 5 E). As a result, we discovered the increasing moment of neuronal signal to be the moment of food search initiation (Figure 5 F, G, H). Compared to the decreasing activity of AgRP neurons on search behavior onset, LepR neurons showed increasing activity (Fig 5 I). If LepR neurons were to be the secondary neuron driving feeding behavior that activates subsequently to AgRP neurons, we hypothesized that neuronal onset would occur immediately after AgRP inactivation. Examination of the neuronal onset of LepR neuron showed activation approximately at 4s before the initiation of the search phase (Fig 5 J, K, L). We then investigated the temporal dynamics of LepR neurons during the approach test (Fig 5 M). Neural activity showed robust increase when specifically approaching food, but Z-score changed specifically when food was available (Fig 5 N, O, Q). The max z-score of unobtainable food condition was half the obtainable food, decreasing momentarily after the termination of the approach phase (Fig 5 P). These results show that activation of LepR neurons occur before voluntary motivated food search initiation. This is subsequent to the deactivating temporal dynamics of AgRP neurons at voluntary food search initiation. Overall, our results show that LepR neurons directly drive sustained food seeking behavior after AgRP deactivation.

Artificial Activation of LH LepR Neurons Drive Food Search and Food Approach

Given that activity of LH LepR neurons had direct and instant causalities of search phase behavior in multi-phase feeding behavior (Fig 6), we next sought to identify whether stimulation of LH LepR neurons induce search phase in ad-libitum mice. To quantify food search bouts, we performed chemogenetic activation in mice during the hidden palatable food test (Fig 6 B) which had been specially designed to distinguish food search behavior.

During the test, mice were well trained for several days to dig the edges of each corner to find palatable food. Food was not placed in the food zone at experimental day on purpose to measure search phase specific behavior. Tracking of mouse showed increased visits and overall movement to food zone when injected with CNO (Fig 6 C). We then defined search behavior into three categories (A: Digging with paw, B: Digging or sniffing with nose C: Sniffing the white floor) to quantify the amount of searching bouts in the food zone. Based on our definition, raster plot of mice showed increased searching bouts when injected with CNO (Fig 6 E). The total search duration was significantly increased in CNO injected mice compared to saline injection (Fig 6 D). CNO injected mice showed increase in search duration per bout and latency to the first search behavior compared to saline injected mouse (Fig 6 D). We next examined effects of approach phase during chemogenetic modulation of LHA LepR neurons. Activation of LepR neurons with CNO injection significantly increased duration in food zone (Fig 6 F G H). Consistently, chemogenetic inhibition of LH LepR neurons with 4Di showed decrease duration in food zone and object zone. The ratio percentage to stay in the food zone compared to duration in whole zone also increased. (Fig 6 I). These chemogenetic results show that LepR neuronal activation is sufficient for food search and food approach.

NPY Application to LH LepR Neurons Significantly Increase Activity

To figure out the source of sustained activity of LH LepR neurons in fiber photometry experiment, we performed the slice calcium imaging with drug application. It has been suggested that NPY is one of the neurotransmitters released from AgRP neurons. We assumed NPY as a candidate of neural determinants by which AgRP neurons activate LepR neurons. To examine whether LH LepR neurons respond to NPY, we acquired calcium image data before and after NPY bath application. We used the mice which were verified to show increased activity during food seeking behavior (Fig 7). When NPY was applied to LH LepR neurons 5 minutes after the baseline period, calcium signals of these neurons were significantly increased compared to the baseline period. (Fig 7 B). Z-score of 5 out of 16 individual neurons showed increase after NPY application. Threshold of z-score 0.2 value categorized neurons that increased with application of NPY (Fig 7-C). Here, we confirmed that LH LepR neurons are activated by NPY.

4. Discussion

The present study demonstrated temporal dissociation between ARC AgRP neuron activity and feeding behavior. These results indicate that AgRP neuron drive feeding behavior through an indirect and delayed causality mechanism. Photometry study showed that ARC AgRP neurons are spontaneously deactivated before feeding behavior initiation. In addition, multi-phase feeding behavior was sustained after AgRP deactivation. Evidence of an indirect and delayed causality mechanism was also shown in AgRP optogenetics studies. Immediate behavior response could not be observed, after artificial activation initiation. Sustained behavior response was observed, after artificial activation termination. These ARC AgRP results suggest that there should be a secondary downstream neuronal population

which directly and immediately drives multi-phase feeding behavior after deactivation of ARC AgRP neurons. The present results regarding LHA LepR neurons suggest that the LHA LepR could be the secondary neurons driving multi-phase feeding behavior. LHA LepR neurons are activated before feeding behavior initiation and sustain its activity throughout the multi-phase feeding behavior. Artificial activation of LHA LepR neurons increases multi-phase feeding behavior. Slice calcium imaging results showed the possibility that NPY from the AgRP neurons could be the downstream neuromodulator of AgRP neurons, driving LH LepR neuron activation. Taken together, these results clarify the paradoxical mystery of temporal dissociation of ARC AgRP neurons and feeding behavior. These results provide the first evidence that LH LepR neurons are the downstream circuit of ARC AgRP neurons directly driving feeding behavior.

Novel developed experimental paradigms, which were designed to dissect the neuronal temporal dynamics according to specific behavior phases, elucidated the role of ARC AgRP → LH LepR circuit in multi-phase feeding behaviors. For the first time, our special experimental design made it possible to investigate the voluntary food search initiation of mice. In previous similar studies[7, 8], food was passively provided to the mice by the experimenter. However, in our study, the mice could make voluntary decision of when to initiate food search behavior. Due to this unique advantage, we could investigate the neuronal activity change before, during and after voluntary behavior initiation for the first time.

Our novel results on the AgRP neurons show that AgRP neurons do not directly and temporally control food seeking behavior. Many reports on AgRP neurons have shown that they are deactivated after food discovery[7-9, 36]. There have also been results of AgRP neurons deactivating with the presentation of visual cues by receiving signals from the insular cortex[29]. These studies suggested that AgRP neurons encode future prediction of energy homeostasis. Since future prediction of energy deprivation is greatly altered by food discovery, AgRP neurons are deactivated by the food discovery. The present study provides the first evidence that the AgRP neurons are deactivated even before the food search initiation, which is far earlier than food discovery. Correspondingly, in the AgRP neuron optogenetic stimulation tests, the temporal quantification results of specific behaviors demonstrated an absence of behavior with a latency of several minutes after stimulation. The present results are strong evidence that the AgRP neurons are not the direct and immediate driver of feeding behavior. Furthermore, these results indicate that AgRP neurons may induce the craving phase acting as preparatory neurons, facilitating an unknown secondary downstream neuron, which is the direct and immediate driver of feeding behavior.

Until now, the role of LH LepR neurons (a sub-population of LH GABA neuron) on feeding behavior have not been fully explored. Recent studies showed that LH LepR neurons increase food related behavior [27], but casual activity and the direct mechanisms of LH LepR neurons have not been showed. Here, our results show for the first time that LH LepR neurons start to activate even before search initiation and escalate further during approach to food specifically. Chemogenetic results also showed increased food search and food approach, suggesting that LepR neurons drive feeding behavior during the search phase and the approach phase.

We also show for the first time that POMC neurons activate later than the sensory detection of food during consumption of food. Reports have shown that POMC neurons activate with the discovery of food[7] [12],, but our results show POMC neurons activating on approach to food, then escalating during food consumption. These results show that POMC activation during food consumption must be specifically observed innately regarding the

relationship between the gut and the brain[12],.

These are the proposed causality mechanisms (Figure 6-D). (1) Energy deprivation state causes AgRP neuron activation (increased NPY concentration in LH). (2) Increased NPY neuromodulation causes increased excitability of LepR - inhibitory interneuron double negative feedback local-circuit, which makes the local-circuit in preparatory mode (ready to start excitation, but not yet received the starting excitation). (3) As the animal decides to initiate food seeking voluntarily, cortex neurons send the starting excitation signal to the local LepR circuits. Since the local-circuit was in high excitability state (ready/preparatory mode), this starting excitation signal can activate the local-circuit to "On mode". The "On mode" can be sustained for substantial duration (~10 seconds) by the double negative feedback mechanism (LepR-interneuron local-circuit acting as a flip-flop on-off switch). (4) The sustained LH LepR neuron activation indirectly drives dopamine release in VTA, which drives the food seeking behavior. (5) As soon as the animal decides to start feeding behavior and detect cues related to upcoming food, the animal recognizes that it will soon eat food. (6) Cognition of near future upcoming food inhibits AgRP neuron (AgRP encodes future prediction of energy status, suggested by previous studies[7, 9, 29].

These results and proposed mechanisms suggest that “ARC AgRP neuron → LH LepR neuron” circuit act as a “preparatory neuron → execution neuron” circuit for feeding behavior. ARC AgRP neurons are mainly active during craving phase and delivers preparatory signal (NPY) to downstream LH LepR neurons. When sufficient NPY is delivered to LH, LH LepR neurons are ready to be activated by decisional signal from the cortex. After initial activation, LH LepR neurons sustain its activity throughout the search phase and approach phase, directly driving search and approach behavior.

In conclusion, the present study suggest that LH LepR neurons directly drive sustained food seeking behavior after AgRP neuronal deactivation via neuromodulation of NPY. This new mechanism could unravel the role of diverse neurons encoding transition between food craving and food seeking phases and may guide novel therapeutics for obesity and eating disorder.

5. Method

Animals

All experimental protocols were approved by Seoul National University, IACUC following the Seoul National University Institutional Animal Care and Use Committee, and were performed according to Health guidelines for Care and Use of Laboratory Animals from the Seoul National University. Mice were housed on a 08:00 to 20:00 light cycle with standard mouse chow and water provided ad libitum, unless otherwise noted. For all behavioral experiments, adult male mice (at least 8 weeks old) were used, and behavior tests were conducted in the behavior chamber during the light cycle.

Stereotaxic Viral injections

Cre recombinase-expressing mouse lines and the cre-dependent AAV vectors were used. AgRP-cre and POMC-cre mouse were injected with virus to study the arcuate nucleus (ARC), Vgat-cre and LepR-cre mouse were injected with virus to study the lateral hypothalamus (LH). Mice were anesthetized with xylazine (20 mg per kg) and ketamine (120 mg per kg) in saline and placed into a stereotaxic apparatus (KOPF or Stoelting).

For fiber photometry experiments, a pulled glass pipette was inserted into the target site; the arcuate nucleus (ARC, 300nl total) at the coordinates (AP: -1.3 mm, ML: ±0.2 mm, DV: 5.85mm from bregma for AgRP mice and AP: -1.4 mm, ML: ±0.2 mm, DV: 5.85mm from bregma for POMC mice) and the lateral hypothalamus (LH, 400nl total) at the coordinates (AP: -0.8 mm, ML: ±1.1 mm, DV: 5.25mm from bregma for Vgat mice and AP: -1.5 mm, ML: ±0.9 mm, DV: 5.25mm from bregma for LepR mice). After 10min, the GCaMP6 virus (AAV1.Syn.Flex.GCaMP6s.WPRE.SV40, Addgene; titer 1.45x10^13 genome copies per ml with 1:2 dilution) was injected unilaterally for 10min using a micromanipulator (Nanoliter 2010). Following infusion, the glass pipette was kept at the target site for 10min and then withdrawn slowly.

For optogenetic experiments, opsin virus (AAV5.EF1a.DIO.hChR2(H134R).EYFP, Addgene; titer 2.4x10^13 genome copies per ml) was injected into ARC bilaterally (300nl, AP: -1.3 mm, ML: ±0.2 mm, DV: 5.85mm from bregma for AgRP mice) and into LH bilaterally (400nl, AP: -1.5 mm, ML: ±0.9 mm, DV: 5.25mm from bregma for LepR mice).

For chemogenetic experiments, DREADD virus was injected into LH bilaterally at the same coordinate for LepR mice (AAV8.hSyn.DIO.hM3D(Gi).mCherry, Addgene; titer 1.9x10^13 genome copies per ml and AAV8.hSyn.DIO.hM3D(Gq).mCherry, Addgene; titer 4.8x10^12 genome copies per ml).

Optical fiber/Cannula implantation

On the same day as virus injection surgery, optical fiber was inserted. Optical fiber implantation was performed after 30min virus injection to prevent backflow.

For fiber photometry experiments, a ferrule-capped optical cannula (400um core, NA 0.57, Doric Lenses, MF2.5, 400/430-0.57) was unilaterally placed 0-50 um above the virus injection site (as previously described) and attached to the skull with Metabond cement (C&B Super Bond).

For optogenetic activation of AgRP neurons, a unilateral optical fiber (200um core, NA 0.37, Doric Lenses, ZF1.25_FLT) was implanted 100um above the ARC injection site and secured to the skull with Metabond cement. For optogenetic manipulation of LepR neurons, optic fiber implantation was bilaterally conducted 100-500um above the LH injection site at a 10º angle from vertical in the lateral to medial direction and affixed to the skull with Metabond cement.

Before or after surgery, dexamethasone, ketoprofen, and cefazolin were injected for postoperative care. All mice were recovered in their cages for at least 2 weeks before the behavioral experiment. Mice were handled for 5 consecutive days to relieve stress and acclimated to the behavior chamber for 30min before testing.

Food Restriction

During the behavioral experiment, all mice were single caged for food restriction, and their food was restricted to maintain 80-90% of initial body weight at fed state. Daily body weight was monitored at the same time each day. After experimentation, mice were placed in a new cage with clean bedding and consumed chow aliquot (0.5~3.0g) to maintain their body weight.

Fiber Photometry

To monitor neuronal calcium activity, fiber photometry system from Doric Lenses was ~~performed~~ required. 465 nm and 405 nm LED light sources (Doric LED Driver) were delivered continuously through a rotary joint (Doric Lenses, FRJ_1X1_PT-400/430/LWMJ-0.57_1m) connected to the patch cord (Doric Lenses, MFP_400/430/1100-0.57_1m) and the GCaMP6 signal was collected back through the same fiber into the photodetector (Doric Lenses). Fiber photometry recordings with two excitation wavelengths: 405 nm measures excited GCaMP fluorescence at isosbestic point and 465 nm measures calcium-dependent GCaMP fluorescence, a proxy for neural activity. The signals were amplified and converted to digital signal through an amplifier, the fiber photometry console respectively. Converted digital signal was recorded at Doric Studios using “Analog in” function. All fiber photometry experiments were conducted after photobleaching (at least 1 hour) to minimize artifact signals.

Prior to experimentation, all mice were habituated to the experimental cages and fiber handling was conducted for at least 3 days. Positive control test was performed to confirm the successful signal of the GCaMP. After 5 minutes of habituation stage, mice were given 1 chow pellet and neuronal activity change was monitored. The mice that did not show any activity change during the positive control test were not used for the behavioral experiment. Fiber photometry signal were time locked with video recordings with Ethovision system.

Fiber Photometry Recording During Multiphasic Feeding Behavior

Multi-phase Feeding Test

“L” shape chamber was specially made with acryl, shaped with one long corridor for observation of multi-phase feeding behavior. The length of the corridor was 60cm and the width 8.5cm. At the edge of the chamber corridor, a red color shelter (6cm x 12cm x 18cm triangle box) was placed with bedding in order to give mice security. Observation was recorded on the moment mice left the shelter to search for food. To block the visual food cue and elongate the approach phase, an arch bridge was placed at the beginning of the food zone.

The Multi-phase Feeding Test was comprised of 3 phases: Food search, Food approach, Food consumption. To accurately assort 3 phases and monitor calcium signals at initiation of each phase, we defined 3 criteria for the moment of the phase transition: Search initiation (The moment of transition from craving to search), Discovery (From search to approach), Food contact (From approach to consumption). We defined the moment when mice left the shelter and ran straight to the food zone as “Search initiation”. The moment that the mice were located on the top of the bridge when the mice visually detected the food was defined as “Discovery”. “Food contact” was defined as the moment when the mice contacted food. Each trial started when a door was opened with scheduled timing from the experimenter.

Before the experiment, choco-pellet (20mg) were given to the mice to minimize food neophobia. Mice were sufficiently habituated at the chamber to be familiarized with shelter and bridge by giving the choco-flavored pellet at the food zone. The experiment was performed across three days in a fasted state. On day 1, no food sessions (the food was not in the corner of the food zone) were performed for 3 trials to confirm neuronal activity in the natural state of not knowing that there is food in the food zone. Food sessions were performed for 15 trials to let the mice know the location of the food zone. On day 2, 15 trials of food sessions were performed for conditioning of the food zone. On day 3, no food session and food session were conducted. Each trial was finished after mice entered the food zone and went back to the shelter. The scent of food was saturated in the behavior chamber to minimize the effect of smell during the behavior test.

Search Test

The phase transition to search for food is an important timing in feeding research. There are many studies of appetitive phase, most being studies of the approach phase (behavior toward already presented food) [7, 25], but there have been few studies specific to search phase (behavior toward invisible food based on memories or habits). Especially, it is difficult to observe 'voluntary' search behavior because of passive presentation from experimenters (2015 Chen). We devised a novel Search Test to observe voluntary search behavior, using a specially made chamber (30cm x 30cm square shape chamber with narrow corridor, 6cm). This test mimicked the environment of a mice in a cave, running to search for food despite the risk of fear outside, such as predatory threat. The cave is emulated with a red color shelter (6cm x 12cm x 18cm triangle box), and the fear outside were implemented with shock conditioning. Mice learned that the food always existed at the end of the corridor, in order to search for food, not roam without purpose. In other words, the mice were let to weigh between the threat outside and motivation for food in its shelter. When motivation for food is higher than the fear of going outside, the mice stepped outside of the shelter to search for food. We defined this moment as "Search Initiation".

Before the experiment, choco-ring aliquot (OREO OZ, 1/8 aliquot; 0.2g) were given to the mice to remove effects of food novelty. Mice were sufficiently familiarized at the specialized chamber. The experiment was performed across seven days on average (five-ten days depending on the learning rate of mice) in a fasted state. On day 1, food zone conditioning was conducted so that mice learned the presence of the choco-ring was at the end of the corridor. The mice performed the task for 20-25 trials in average; Until the mice was full. On day 2-6, food zone conditioning was conducted with shock conditioning (random shock; shock omission 7s, mean 0.03mA shock with 10s interval). The task was performed for 20-25 trials in average. On day 7, test session was conducted with shock. All trials were used for analysis regardless of the presence or absence of shock at search initiation to food. There was no change of calcium signal for the effect of shock in AgRP, POMC, LepR mice.

Vertical approach test

Approach Test was performed to monitor calcium signal during approach to food which had been presented beforehand. However, it was difficult to observe signals during the approach phase due to few problems. The approach phase lasted momentarily, not even lasting a second and food undirected movement of mice also made it vague for the experimenter to judge the intention of the mouse. To resolve this problem, we designed a Vertical approach test using a short L corner box. This devised test made elongated approach phase and definite observation of food directed behavior possible.

Approach test comprised of two sessions; food placement at height of 10cm or 12cm.

Choco-ring aliquot (OREO OZ, 1/8 aliquot; 0.2g) was placed in the tray at one side of the wall. During session at a height of 10cm, the mice approach and successfully obtain the food, followed by initiation of food consumption. During session at a height of 12cm, the mice could approach, but not obtain the food. Thus, this session isolates food consumption from the approach phase. The approach behavior had three sequential behaviors; Rearing Up, Rearing Moment (or Food contact), Rearing down. The point when the mice raised its paw was defined as “Approach Initiation”. The point when mice contact food (Food contact) or the paramount height mice could reach to get the food (Rearing moment) was also recorded, and the point when the mouse stepped down (Rearing down) was recorded manually.

The experiment was performed for a day in fasted state. To monitor the baseline of GCaMP signals, the signals from mice were recorded beforehand for about 3 min. Following the recorded baseline, choco-ring aliquot was placed in the 10cm tray which was followed by the 12cm tray. Each session was performed until the mice conducted 8 trials of approach behavior.

Contact Test

Contact test using the L-shaped chambers were performed for tests with inedible objects (Lego) and Choco-flavored snacks. During the first five minutes, Lego was placed at a corner of the chamber. A door which was placed to block mice from food was removed five seconds after recording onset to let mouse freely move towards food. Subsequently in the food presentation session, the choco-flavored snacks were presented at intervals of two minutes after removing the previous object from the chamber. During the next five minutes, choco-flavored snacks were placed at the corner of the chamber. And then, it was conducted in the same way.

Photostimulation

Photostimulation of AgRP neurons was conducted with 473nm laser (Shanghai) delivered through FC-FC monofiberpatchcord (Doric Lenses) to the rotary joint and then, FC-ZF 1.25 monofiberpatchcord to the cannula (Doric Lenses, 200/220/0.23). Laser intensity for activation was approximately 10mW at the tip. The console (Doric Lenses) was used to generate laser pulse. Optogenetics stimulation protocol consisted of light pulses (10 ms) for 1 s at 20 Hz flowed by a 3-s break. Before photostimulation experiments, laser was emitted before the experiment for at least 30 min to stabilize its function. The mice were tracked using EthoVision XT 10 (15) (Noldus).

Photostimulation During Multiphasic Feeding Behavior

Open field test for food intake measurement

Mice were gently placed at the open field test box (32cm x 32cm x 32cm) while a chow was placed at the center of the chamber. The experiment was performed across three days in fed state (day 1: laser off Day2: laser on Day 3: laser off) to ensure infection of ChR2 at the ARC. Food intake was measured after 30 min of experiment

Open field test for behavior analysis

Mouse was gently placed at the Open Field Test box with a chow. Session were divided into pre-stimulation, stimulation, and post stimulation to quantify behavior change before and after optogenetic laser stimulation. Each session was performed for 10 minutes. Feeding bouts were manually scored using a side view camera.

The area was divided into nine and the chow was place at the center of it, which was defined

as the food zone.

Vertical Approach Test

The laser was stimulated for 5 min respectively. All mice were fed state during experiment. At each sided of the open field box, choco-flavored snack and control was placed at a height of 11cm where the mouse should rear up to get food. The rearing behavior was measured manually or with Ethovision (Noldus).

Chemogenetic manipulation

Mice had ad libitum access to water and food, and all test sessions were conducted during the light period. For Hidden palatable food search test, LH LepR neurons were injected with AAV8-hSyn-DIO-hM3Dq-mCherry virus. For Horizontal Approach test, AAV8-hSyn-DIO-hM3Dq-mCherry/AAV8-hSyn-DIO-hM4Di-mCherry were injected to LH LepR cre mice.

Chemogenetic manipulation During Multiphasic Feeding Behavior

Horizontal Approach Test

Cube sugar (food) and cube clay (false food) were diagonally placed into the each corner of chamber. Clozapine-n-oxide (Sigma, CNO, 1mg/kg, *i.p.*) or vehicle (Saline, *i.p.*) was administered before 1hr in ad-libitum mice. During test sessions, mice would explore and approach to the food or false food. For analyzing zone duration time and heatmap visualization,we used Ethovision XT 14 (Noldus) software.

Hidden-Food Search Test

Mice were acclimated three times in an open field box before conditioning session. For the conditioning session, two raisins were hidden under wood bedding at each edges of the corner. Twice a day (three consecutive days) mice were let to search the box for hidden raisins during 10mins of experiment. On behavioral experimental day, clozapine-n-oxide (Sigma, CNO, 1mg/kg, *i.p.*) or vehicle (Saline, *i.p.*) was administered before 1hr. For quantification of search behavior, we defined search behaviors into three categories which are as follows: (A) Digging with paws (B) Digging/Sniffing with nose (C) Sniffing the white open field box floor. These behaviors were analyzed by Observer XT 13 (Noldus). Behavior track and zone duration analysis were done with Ethovision XT 14(Noldus).

Histology, Immunohistochemistry, and Imaging

At the termination of behavior experiments, mice were deeply anesthetized with xylazine and ketamine in saline. Transcranial perfusion was performed with phosphate-buffered saline (PBS) followed by 4% neutral buffered paraformaldehyde (T&I, BPP-9004). Brains were extracted, and post-fixed in 4% paraformaldehyde at 4℃, and transferred to 10% sucrose followed by 30% sucrose for cryoprotection. Cryoprotected brains were sectioned coronally on cryostat (Leica Biosystems, CM3050) at 50 um and their sections were stained with 4',6-diamidino-2-phenylindole (DAPI) to visualize nuclei. To verify scientific exactitude, fluorescent images of viral fluorescence, fiber/cannula placements were captured with a confocal microscope (Olympus, FV3000).

Preparations of brain slice and Slice calcium imaging

Brain slices were obtained from anesthetized (C57BL/6 male) mice at least 3 weeks after virus injection. Lateral hypothalamus slices were dissected into 250 μm thickness using a vibratome (Leica, VT1200S) in ice-cold standard artificial CSF (aCSF) containing the following (in mM): 125 NaCl, 2.5 KCl, 1 $MgCl_2$, 2 $CaCl_2$, 1.25 NaH_2PO_4, 26 $NaHCO_3$, and 25 glucose bubbled with 95% O_2 and 5% CO_2. For recovery, slices were incubated at 32°C for 30 min and then a further 1 hour at room temperature. Then the slices were transferred to

the recording chamber and perfused with aCSF at 32°C during imaging. Calcium measurements were performed with a CMOS camera (Photometrics, USA) attached to an upright microscope (BX50WI, Olympus) using a 40X or 10X water-immersion objective (NA 0.8 or 0.3, LUMPlanFL N or UMPlanFl; Olympus) at 10 frame per second. A broad white light source (CoolLED, pE-340 fura, USA) was passed through an excitation filter (450-480 nm) and collected through an emission filter (525/50 nm). Fluorescence images were acquired with VisiView software (Visitron Systems GmbH, Germany).

Drugs

Neuropeptide Y (NPY) was purchased from Tocris. NPY was dissolved with aCSF (400 μM) for slice application. Final concentration of the drug used in the calcium imaging experiments was as follows: 1 μM.

QUANTIFICATION AND STATISTICAL ANALYSES

All photometry data analysis was done with Matlab 2019A and PrismPad.

Fiber Photometry Data Analysis

Fiber photometry data was received and filtered with Doric Console. F/F0 was calculated as (465nm-405nm)/fitted(405nm) [37]. Z-Score and SEM was calculated with Matlab. Heatmap was made by calculating each normalized trials with the following formula. (Z-score-min(Z-score))/Max(Z-score)-Min(Z-score). Heatmap trials were aligned to each of its time of max z-score except for the approach test which were aligned in experimentally proceeded order (Fig 4).

Behavior Data Analysis

Behavior data analysis were conducted manually frame by frame in 30 frames per second using behavioral observation tool (Observer XT ver.15 and Ethovision ver.14). All videos were taken at a 30Hz frame rate with high resolution. Signal recordings and each of the videos recorded were synchronized to visualize behavior in the same experiment. A red laser was emissioned at start of experiment to set synchronized set point. The exact time of behavior on frame was calculated and quantified for each behavior moment before analysis with MATLAB.

Statistical Analysis

All statistical data was analyzed with MATLAB or IBM SPSS 25.0. Data are reported as mean ± SEM in the figures. t-test was conducted for comparisons between two groups. Two-Way repeated measures ANOVA was done for multiple testing conditions. p values for comparisons across multiple groups were corrected using the Greenhouse-Geisser method in IBM SPSS 25.0. □p < 0.05. □□p < 0.01, □□□p < 0.001, □□□□p < 0.0001.

Slice Calcium Imaging Data Analysis

The ROIs were manually detected in a field of view (in the LHA area), and signals were preprocessed by using exponential fit for fluorescence bleach correction. Background fluorescence was subtracted and converted to dF/F0 value. The value of F0 was calculated using the value of the 10 percentage in a baseline period. All calcium imaging data analysis was done with ImageJ.

6. Legend

Figure 1 Diagram of Multi-Phase Feeding Behavior

Figure 2 ARC Neurons Show Distinct Temporal Dynamics of Feeding Behavior

(A) Histology of AgRP or POMC mouse showing injection site and optical fiber.

(B) Schematic of the multi-phase feeding test apparatus with a mouse and a shelter.

(C) Representative calcium signals from AgRP and POMC neurons during the multi-phase feeding test aligned to the time of search initiation. Animals were video-traced and trial initiation (red) search (orange) approach (green) consumption (blue) behaviors were visually scored.

(D) Mean percentage − SEM of ARC AgRP or POMC neuron activity patterns across multi-feeding behavior (color-coded bar, *upper*).

(E) Heatmap of AgRP and POMC neuron activity during the multi-phase feeding Test (n=15 trials per mouse, AgRP: 6 mice, POMC: 4 mice). Each row is a single trial of AgRP or POMC GCaMP6s mouse.

(F) Cartoon of the search test apparatus with a mouse and a shelter.

(G) Mean Z-score of ARC AgRP and ARC POMC calcium response during search initiation (AgRP: 4 mice , POMC: 4 mice).

(H) Individual Z-scores of AgRP (*left)* or POMC (*right*) calcium response for before (-5 to -4s) and after (4 to 5s) search behavioral onset (repeated-measures ANOVA, AgRP $F(1,49)=25.738$, $P<0.001$; POMC $F(1,68)=0.199$, $P=0.657$) (AgRP: n= 53 trials, N= 4 mice) (POMC: n= 72 trials, N= 4 mice).

(I) Heatmap of ARC AgRP and ARC POMC neuron activity during search initiation (AgRP: n= 53 trials, N= 4 mice) (POMC: n= 72 trials, N= 4 mice). Each row is a single trial of AgRP or POMC GCaMP6s mouse.

(J) Illustration of signal onset (dashed red line) relative to search initiation onset (dashed black line) using the third methods.

(K) Cumulative probability distribution and Histogram (relative probability distribution) of the AgRP neuron signal onset during search test (AgRP: n= 53 trials, N= 4 mice).

(L) Signal onset relative to search initiation of ARC AgRP Neuron. Signal onset occurred at −6.656 ± 0.465s ($P < 0.0001$ by two-tailed one-sample t test; t, df = 14.30, 5).

(M) Cartoon of the approach test apparatus with a mouse.

(N) Mean Z-score of AgRP calcium response during approach test aligned to approach initiation (green: obtainable food, yellow green: unobtainable food) (N= 4 mice).

(O) Representative calcium signals of AgRP neurons aligned to the time of approach

initiation at obtainable food (*left*) or unobtainable food (*right*) (green: rearing up, red: food contact, blue: consumption initiation).

(P) Individual Z-score of AgRP neurons aligned to the time of approach initiation at obtainable food (*left,* n=32 trials, N=4 mice) or unobtainable food (*right,* n=29 trials, N=4 mice) (obtainable food : repeated-measures ANOVA, baseline versus 0-1s, $F(1,28)=4.9871$, $p=0.034$; baseline versus 1-2s, $F(1,28)$, $p<0.0001$; baseline versus 14-15s, $F(1,28)=2.9977$, $p=0.094$) (unobtainable food : repeated-measures ANOVA, baseline versus 0-1s, $F(1,25)=23.5086$, $p<0.0001$; baseline versus 1-2s, $F(1,25)$, $p=0.086$; baseline versus 14-15s, $F(1,25)=12.283$, $p=0.002$) .

(Q) Mean Z-score of AgRP calcium response during approach test aligned to approach initiation (green: obtainable food, yellow green: unobtainable food) (N= 4 mice).

(O) Mean Z-score of POMC calcium response during approach test aligned to approach initiation (green: obtainable food, yellow green: unobtainable food) (N= 4 mice).

(R) Representative calcium signals of POMC neurons aligned to the time of approach initiation at obtainable food (*left*) or unobtainable food (*right*) (green: rearing up, red: food contact, blue: consumption initiation).

(S) Individual Z-score of POMC neurons aligned to the time of approach initiation at obtainable food (*left,* n=32 trials, N=4 mice) or unobtainable food (*right*, n=30 trials, N=4 mice) (obtainable food: repeated-measures ANOVA, baseline versus 0-1s, $F(1,26)=13.708$, $p=0.001$; baseline versus 1-2s, $F(1,26)=43.64$, $p<0.0001$; baseline versus 14-15s, $F(1,26)=32.952$, $p<0.0001$) (unobtainable food: repeated-measures ANOVA, baseline versus 0-1s, $F(1,28)=3.823$, $p=0.06$; baseline versus 1-2s, $F(1,28)=34.85$, $p<0.0001$; baseline versus 14-15s, $F(1,28)=0.0002$, $p=0.988$).

Solid lines represent the average, and shaded areas indicate the S.E.M.

Data are reported as mean ± S.E.M.

Figure 3 Artificial Activation of AgRP Neurons Does Not Immediately Drive Feeding Behavior and Feeding Behavior is Sustained after Artificial Deactivation of AgRP

(A) Schematic view of AgRP mice showing virus and optical fiber injection. Cre dependent Chr2 was injected unilaterally to ARC using AgRP-cre mouse.

(B) Chow consumption for 30min (N=7 mice) (Paired t-test, Day1 vs Day2 ;$p<0.0001$, Day2 vs Day3 ;$p<0.0001$, Day1 vs Day3 ;$p= 0.155$).

(C) Experimental design. The laser stimulation was applied for 1 second followed by a 3 second break repeatedly for 10min. Frequency was 20hz with 10ms pulse. Mouse behavior was recorded with synchronized camera at the top and side.

(D) Representative heat map and track encoding spatial location of an AgRP::ChR2 mouse during off-on-off stimulation protocol.

(E) Representative data of feeding behavior during off-on-off simulation protocol.

(F) Mean time of latency to start food intake during laser stimulation (blue) or latency to terminate food intake at post photo stimulation (gray).

(G) Raster plot of feeding patterns of AgRP mice during 10 min off-on-off stimulation. Each row represents an individual mouse (black bar: feeding behavior, blue shadow: laser stimulation).

(H) Histogram and cumulative distribution of feeding duration in time bins of 1 min (black bar: feeding duration time, red line: cumulative distribution, blue shadow: laser stimulation).

(I) Probability of distance from a mouse to food in 1st 1min (red) or last 1min (blue) during photo stimulation (left) or post stimulation (right) (bar graph: relative, line graph: cumulative distribution) N= 6 mice.

(J) Behavior paradigm of effort-needed food approach test.

(K) Heat map encoding spatial location of an AgRP::ChR2 mouse during effort-needed food approach test.

(L) Representative data of an individual mouse behavior during effort-needed food approach test.

(M) The Frequency or duration of food approach during 5 min laser off-on-off (red: non food, blue: food) (paired t test, frequency of food approach: pre vs photo, p; 0.009, photo vs post, p; 0.063, pre vs post, p; 0.095 duration of food approach: pre vs photo, p; 0.007, photo vs post, p; 0.242, pre vs post, p; 0.066) (paired t test, frequency of non food approach: pre vs photo, p; 1, photo vs post, p; 0.587, pre vs post, p; 0.477, duration of non food approach: pre vs photo, p; 0.946, photo vs post, p; 0.827, pre vs post, p; 0.893).

(N) Raster plot of approach behavior from an individual mouse during 5min laser off on off stimulation protocol (black bar: food approach)

(O and P) The frequency or duration of food approach in time bins of 1 min (red: control, blue: food).

(Q) Mean time of latency to start approaching behavior during laser stimulation (blue) or latency to terminate approach behavior at post phot stimulation (gray).

Solid lines represent the average, and shaded areas indicate the S.E.M.

Data are reported as mean ± S.E.M.

Figure 4 GABA neurons and LepR neurons show opposing response to Food Contact

(A) Histology of LH GABA or LepR mouse showing injection site and optical fiber.

(B) Cartoon of contact test with a mouse and food (choco-flavored snack) or non food (lego).

(C) Mean Z-Score of LH GABA calcium response aligned to the time of contact (gray: non-food, blue: food) (n= 8 trials per mouse, N=3 mice).

(D) Representative calcium signals from LH GABA neurons at non food contact (left) or food contact (right) (blue bar: food contact to consumption termination, blue tick: consumption start).

(E) Heatmap of LH GABA neuron activity during non food (left) or food (right) contact respectively. Each raw indicates a single trial.

(F) Mean Z-Score of LH LepR calcium response aligned to the time of contact (gray: non-food, blue: food) (n= 8 trials per mouse, N=4 mice).

(G) Representative calcium signals from LH LepR neurons at non food contact (left) or food contact (right) (blue bar: food contact to consumption termination, blue tick: consumption start).

(H) Heatmap of LH LepR neuron activity during non food (left) or food (right) contact respectively. Each raw indicates a single trial.

(I) Delta Z-Score of LH GABA between before (-3 to –2s) and after contact (2 to 3s) of non food or food (paired t test, p=0.03).

(J) Individual Z-scores of LH GABA calcium for before (-3 to -2s) and after (2 to 3s) non food contact (left) or food contact (right) (non food contact repeated-measures ANOVA, F(1,21)= 2.388, p=0.137; food contact: repeated-measures ANOVA, F(1,21)=141.476, p<0.001;) (n= 8 trials per mouse, N=3 mice).

(K) Delta Z-Score of LH LepR between before (-3 to –2s) and after contact (2 to 3s) of non food or food (paired t test, p=0.003)

(L) Individual Z-scores of LH LepR calcium for before (-3 to -2s) and after (2 to 3s) non food contact (left) or food contact (right) (repeated-measures ANOVA, non food contact F(1,28)= 0.109, p=0.743; food contact: repeated-measures ANOVA, F(1,28)=99.228, p<0.001;).

Solid lines represent the average, and shaded areas indicate the S.E.M.

Data are reported as mean ± S.E.M.

Figure 5 Activity of LH LepR Neurons during Search and Approach Phase

(A) Schematic of the multi-phase feeding test apparatus with a mouse and a shelter.

(B and C) Representative calcium signals from LH GABA and LepR neurons during the Multi-phase feeding test aligned to the time of search initiation. Animals were video-traced and craving (red) search (orange) approach (green) consumption (blue) behaviors were visually scored.
(D) Mean percentage − SEM of LH LepR neuron activity patterns across multi-feeding behavior (color-coded bar, Upper).
(E) Cartoon of the search test apparatus with a mouse and a shelter.
(F) Mean Z-score of LH LepR calcium response during search initiation (LepR: 4mice).

(G) Individual Z-scores of LepR (right) calcium response for before (-3 to -2s) and after (2 to 3s) search behavioral onset (repeated-measures ANOVA, F(1,69)= 88.451, p<0.001;) (n= 73 trials, N= 4 mice) .

(H) Heatmap of LH LepR neuron activity during search initiation (LepR: 4mice). Each row is a single trial of LepR GCaMP6s mouse.

(I) Illustration of signal onset (dashed red line) relative to search initiation onset (dashed black line) using the third methods.
(J) Cumulative probability distribution and Histogram (relative probability distribution) of the LH LepR neuron signal onset during search test n= 67 trials, N = 4 mice).

(K) Signal onset relative to search initiation. Signal onset occurred at −5.623 ± 0.418 s ($p < 0.0001$ by two-tailed one-sample t test; t, df = 13.47, 6).

(L) Cumulative probability distribution and Histogram (probability distribution) of the LH LepR or ARC AgRP neuron signal onset during searching test.

(M) Cartoon of the approach test apparatus with a mouse.
(N) Mean Z-score of LepR calcium response during approach test aligned to approach initiation (green: obtainable food, yellow green: unobtainable food) (N= 5 mice).
(O) Heatmap of LH LepR neuron activity during approach phase. Each row is a single trial of LH LepR mouse. *(left*: empty tray, n= 36 trials, N = 5 mice) (*middle*: obtainable food, n= 40 trials, N =5 mice) (*right*: unobtainable food, n= 37 trials, N = 5 mice)
(P) Peak of Z-score during approach phase of empty tray, obtainable food and unobtainable food session, respectively. (paired t test, p=0.021 empty versus obtainable food, p=0.022 obtainable food versus unobtainable food, p=0.03 empty versus unobtainable food)
(Q) Individual Z-scores of LH LepR calcium response for baseline (-3 to -2s) and time bin 1 (0.5 to 1.5s) or time bin 2 (4 to 5s) during approach initiation (gray: empty tray, green: obtainable food, yellow green: unobtainable food tray) (Obtainable food: repeated-measures ANOVA, baseline versus 0.5-1.5s, $F(1,35)=36.368$, $p<0.001$; and baseline versus 4-5s, $F(1,35)=57,881$, $p<0.001$;). (Unobtainable food: repeated-measures ANOVA, baseline versus 0.5-1.5s, $F(1,32)= 35.034$, $p<0.001$;).

Solid lines represent the average, and shaded areas indicate the S.E.M.

Data are reported as mean ± S.E.M.

Figure 6 Activity of LH LepR Neurons during Search and Approach Phase

(A) Representative overview of LH LepR neurons.
(B) Schematic of the hidden food search Test apparatus with a mouse
(C) Heatmap (*left*) Track visualization plot (*right*)

(D) Total search duration (paired t-test p=0.045) (*left*) Search duration per bout (paired t test p=0.093)(*middle*) Latency to first search (paired t-test p=0.019) (*right*) after injection of Saline(Grey) or CNO (Pink) in LH LepR DREADD-Gq mice (n=5) during hidden food search test.

(E) Raster plot (Red: digging with paws. Yellow green: sniffing or digging with nose. Purple: sniffing in white floor)

(F) Schematic of the horizontal food approach Test apparatus with a mouse. Cube clay was placed in zone 1, Cube sugar was placed in zone 2.

(G) Heatmap (*left*) Track visualization (*right*)

(H) Food zone duration (paired t-test p=0.054) (*Left*) Object zone duration (*middle*) Percent time spent in food zone (paired t-test p=0.028) (*right*) after injection of Saline (Grey) or CNO (Pink) in LH LepR DREADD-Gq mice (n=6) during horizontal food approach test.

(I) Food zone duration (paired t-test p=0.065) (*left*) Object zone duration (*middle*)

Percent time spent in food zone (right) after injection of Saline (Grey) or CNO (Purple) in LH LepR DREADD-Gi mice (n=6) during horizontal food approach test.

Figure 7 Calcium activity of LH LepR neurons is activated by Neuropeptide Y application in the acute slice.

(A) Sample traces of spontaneous calcium activity of LH LepR neurons. Yellow circles represent regions of interest (ROIs). The bath application of Neuropeptide Y (1 μM) increased the calcium activity (right, 5~10 min after NPY application).
(B) AUC of calcium activity of LH LepR neurons were significantly increased by bath application of Neuropeptide Y (n = 16, N = 2; *p<0.05, paired t test; a.u., arbitrary unit).
(C) Individual Z-Score and Heatmap of calcium activity in LH LepR neurons. Colorbar changed color from white to blue or red from Z-Score of 0.2. First five neurons are shown in Figure 6-B as representitves (n=16).
(D) Causality mechanisms of ARC AgRP neuron → LH LepR neuron circuit

References

1. Craig, W., *Appetites and Aversions as Constituents of Instincts.* Proc Natl Acad Sci U S A, 1917. **3**(12): p. 685-8.
2. Gong, R., et al., *Hindbrain Double-Negative Feedback Mediates Palatability-Guided Food and Water Consumption.* Cell, 2020. **182**(6): p. 1589-1605 e22.
3. Lee, Y.H., et al., *Food Craving, Seeking, and Consumption Behaviors: Conceptual Phases and Assessment Methods Used in Animal and Human Studies.* J Obes Metab Syndr, 2019. **28**(3): p. 148-157.
4. Aponte, Y., D. Atasoy, and S.M. Sternson, *AGRP neurons are sufficient to orchestrate feeding behavior rapidly and without training.* Nat Neurosci, 2011. **14**(3): p. 351-5.
5. Atasoy, D., et al., *Deconstruction of a neural circuit for hunger.* Nature, 2012. **488**(7410): p. 172-7.
6. Mazzone, C.M., et al., *High-fat food biases hypothalamic and mesolimbic expression of consummatory drives.* Nat Neurosci, 2020. **23**(10): p. 1253-1266.
7. Chen, Y., et al., *Sensory detection of food rapidly modulates arcuate feeding circuits.* Cell, 2015. **160**(5): p. 829-841.
8. Betley, J.N., et al., *Neurons for hunger and thirst transmit a negative-valence teaching signal.* Nature, 2015. **521**(7551): p. 180-185.

9. Mandelblat-Cerf, Y., et al., *Arcuate hypothalamic AgRP and putative POMC neurons show opposite changes in spiking across multiple timescales.* Elife, 2015. **4**.
10. Chen, Y., et al., *Hunger neurons drive feeding through a sustained, positive reinforcement signal.* Elife, 2016. **5**.
11. Chen, Y., et al., *Sustained NPY signaling enables AgRP neurons to drive feeding.* Elife, 2019. **8**.
12. Sternson, S.M. and A.K. Eiselt, *Three Pillars for the Neural Control of Appetite.* Annu Rev Physiol, 2017. **79**: p. 401-423.
13. Fu, O., et al., *Hypothalamic neuronal circuits regulating hunger-induced taste modification.* Nat Commun, 2019. **10**(1): p. 4560.
14. Nieh, E.H., et al., *Inhibitory Input from the Lateral Hypothalamus to the Ventral Tegmental Area Disinhibits Dopamine Neurons and Promotes Behavioral Activation.* Neuron, 2016. **90**(6): p. 1286-1298.
15. Qualls-Creekmore, E., et al., *Galanin-Expressing GABA Neurons in the Lateral Hypothalamus Modulate Food Reward and Noncompulsive Locomotion.* J Neurosci, 2017. **37**(25): p. 6053-6065.
16. Jennings, J.H., et al., *Visualizing hypothalamic network dynamics for appetitive and consummatory behaviors.* Cell, 2015. **160**(3): p. 516-27.
17. Oesch, L.T., et al., *REM sleep stabilizes hypothalamic representation of feeding behavior.* Proc Natl Acad Sci U S A, 2020. **117**(32): p. 19590-19598.
18. Godfrey, N. and S.L. Borgland, *Diversity in the lateral hypothalamic input to the ventral tegmental area.* Neuropharmacology, 2019. **154**: p. 4-12.
19. Arrigoni, E., M.J.S. Chee, and P.M. Fuller, *To eat or to sleep: That is a lateral hypothalamic question.* Neuropharmacology, 2019. **154**: p. 34-49.
20. Petrovich, G.D., *Lateral Hypothalamus as a Motivation-Cognition Interface in the Control of Feeding Behavior.* Front Syst Neurosci, 2018. **12**: p. 14.
21. Qualls-Creekmore, E. and H. Munzberg, *Modulation of Feeding and Associated Behaviors by Lateral Hypothalamic Circuits.* Endocrinology, 2018. **159**(11): p. 3631-3642.
22. Tyree, S.M. and L. de Lecea, *Lateral Hypothalamic Control of the Ventral Tegmental Area: Reward Evaluation and the Driving of Motivated Behavior.* Front Syst Neurosci, 2017. **11**: p. 50.
23. Bonnavion, P., et al., *Hubs and spokes of the lateral hypothalamus: cell types, circuits and behaviour.* J Physiol, 2016. **594**(22): p. 6443-6462.
24. Stuber, G.D. and R.A. Wise, *Lateral hypothalamic circuits for feeding and reward.* Nat Neurosci, 2016. **19**(2): p. 198-205.
25. Li, Y., et al., *Hypothalamic Circuits for Predation and Evasion.* Neuron, 2018. **97**(4): p. 911-924 e5.
26. Leinninger, G.M., et al., *Leptin acts via leptin receptor-expressing lateral hypothalamic neurons to modulate the mesolimbic dopamine system and suppress feeding.* Cell Metab,

2009. **10**(2): p. 89-98.

27. Schiffino, F.L., et al., *Activation of a lateral hypothalamic-ventral tegmental circuit gates motivation.* PLoS One, 2019. **14**(7): p. e0219522.
28. de Vrind, V.A.J., et al., *Effects of GABA and Leptin Receptor-Expressing Neurons in the Lateral Hypothalamus on Feeding, Locomotion, and Thermogenesis.* Obesity (Silver Spring), 2019. **27**(7): p. 1123-1132.
29. Livneh, Y., et al., *Homeostatic circuits selectively gate food cue responses in insular cortex.* Nature, 2017. **546**(7660): p. 611-616.
30. Markowitz, J.E., et al., *The Striatum Organizes 3D Behavior via Moment-to-Moment Action Selection.* Cell, 2018. **174**(1): p. 44-58 e17.
31. Kosse, C., et al., *Orexin-driven GAD65 network of the lateral hypothalamus sets physical activity in mice.* Proc Natl Acad Sci U S A, 2017. **114**(17): p. 4525-4530.
32. Jennings, J.H., et al., *The inhibitory circuit architecture of the lateral hypothalamus orchestrates feeding.* Science, 2013. **341**(6153): p. 1517-21.
33. Hao, S., et al., *The Lateral Hypothalamic and BNST GABAergic Projections to the Anterior Ventrolateral Periaqueductal Gray Regulate Feeding.* Cell Rep, 2019. **28**(3): p. 616-624 e5.
34. Cassidy, R.M., et al., *A lateral hypothalamus to basal forebrain neurocircuit promotes feeding by suppressing responses to anxiogenic environmental cues.* Sci Adv, 2019. **5**(3): p. eaav1640.
35. Mickelsen, L.E., et al., *Single-cell transcriptomic analysis of the lateral hypothalamic area reveals molecularly distinct populations of inhibitory and excitatory neurons.* Nat Neurosci, 2019. **22**(4): p. 642-656.
36. Garfield, A.S., et al., *Dynamic GABAergic afferent modulation of AgRP neurons.* Nat Neurosci, 2016. **19**(12): p. 1628-1635.
37. Lerner, T.N., et al., *Intact-Brain Analyses Reveal Distinct Information Carried by SNc Dopamine Subcircuits.* Cell, 2015. **162**(3): p. 635-47.

LH^{LepR} neuron directly drives sustained food seeking behavior after AgRP deactivation via neuromodulation by NPY

Figure 1

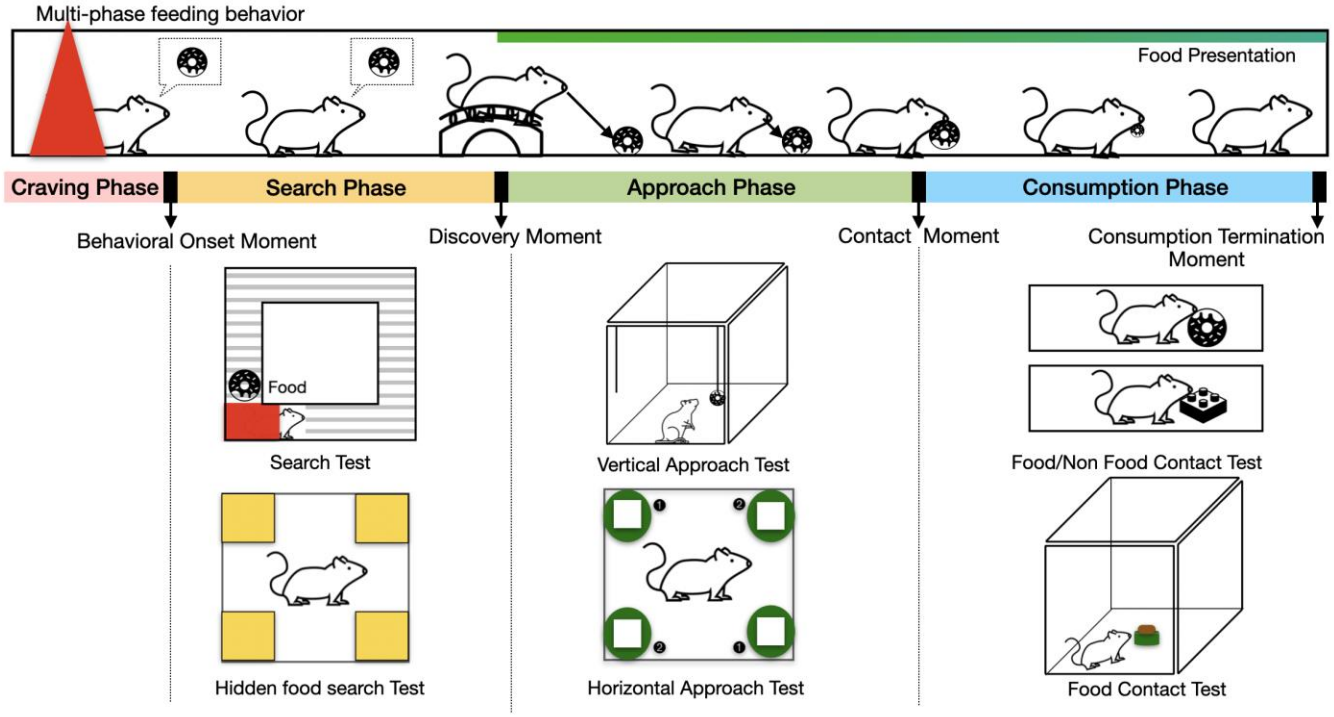
Multi-phase feeding behavior
Food Presentation
Craving Phase
Search Phase
Approach Phase
Consumption Phase
Behavioral Onset Moment
Discovery Moment
Contact Moment
Consumption Termination Moment
Food
Search Test
Vertical Approach Test
Food/Non Food Contact Test
Hidden food search Test
Horizontal Approach Test
Food Contact Test

Figure 2

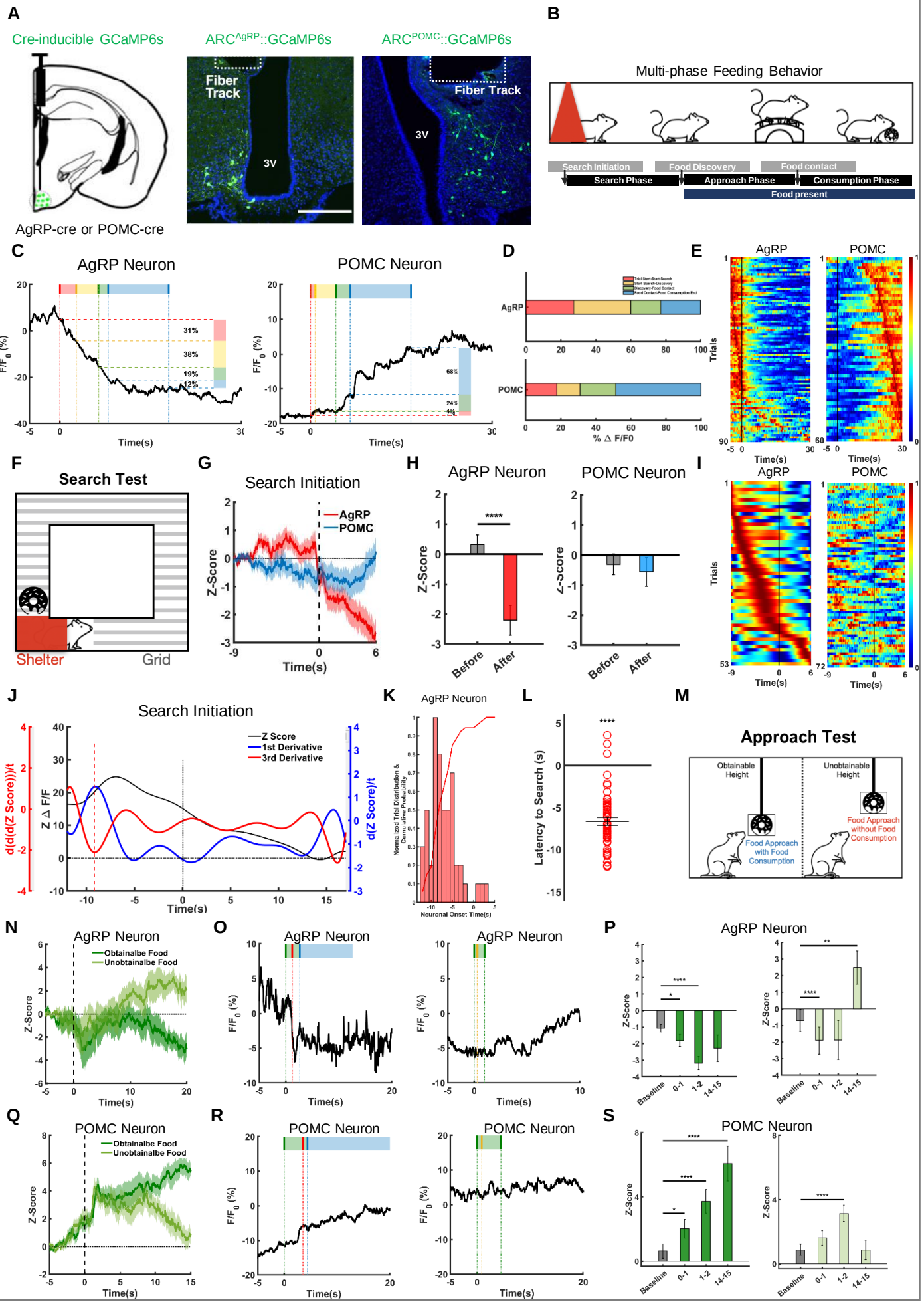
A
Cre-inducible GCaMP6s
ARC^{AgRP}::GCaMP6s
ARC^{POMC}::GCaMP6s
Fiber Track
3V
Fiber Track
3V
AgRP-cre or POMC-cre
B
Multi-phase Feeding Behavior
Search Initiation
Food Discovery
Food contact
Search Phase
Approach Phase
Consumption Phase
Food present
C
AgRP Neuron
POMC Neuron
F/F$_0$ (%)
Time(s)
31%
38%
19%
12%
68%
24%
7%
D
AgRP
POMC
% Δ F/F0
E
AgRP
POMC
Trials
Time(s)
F
Search Test
Shelter
Grid
G
Search Initiation
AgRP
POMC
Z-Score
Time(s)
H
AgRP Neuron
POMC Neuron
Z-Score
Before
After
I
AgRP
POMC
Trials
Time(s)
J
Search Initiation
Z Score
1st Derivative
3rd Derivative
d(d(d(Z Score)))/t
Z Δ F/F
d(Z Score)/t
Time(s)
K
AgRP Neuron
Normalized Trial Distribution & Cumulative Probability
Neuronal Onset Time(s)
L
Latency to Search (s)
M
Approach Test
Obtainable Height
Unobtainable Height
Food Approach with Food Consumption
Food Approach without Food Consumption
N
AgRP Neuron
Obtainalbe Food
Unobtainalbe Food
Z-Score
Time(s)
O
AgRP Neuron
F/F$_0$ (%)
Time(s)
P
AgRP Neuron
Z-Score
Baseline
0-1
1-2
14-15
Q
POMC Neuron
Obtainalbe Food
Unobtainalbe Food
Z-Score
Time(s)
R
POMC Neuron
F/F$_0$ (%)
Time(s)
S
POMC Neuron
Z-Score
Baseline
0-1
1-2
14-15

Figure 3

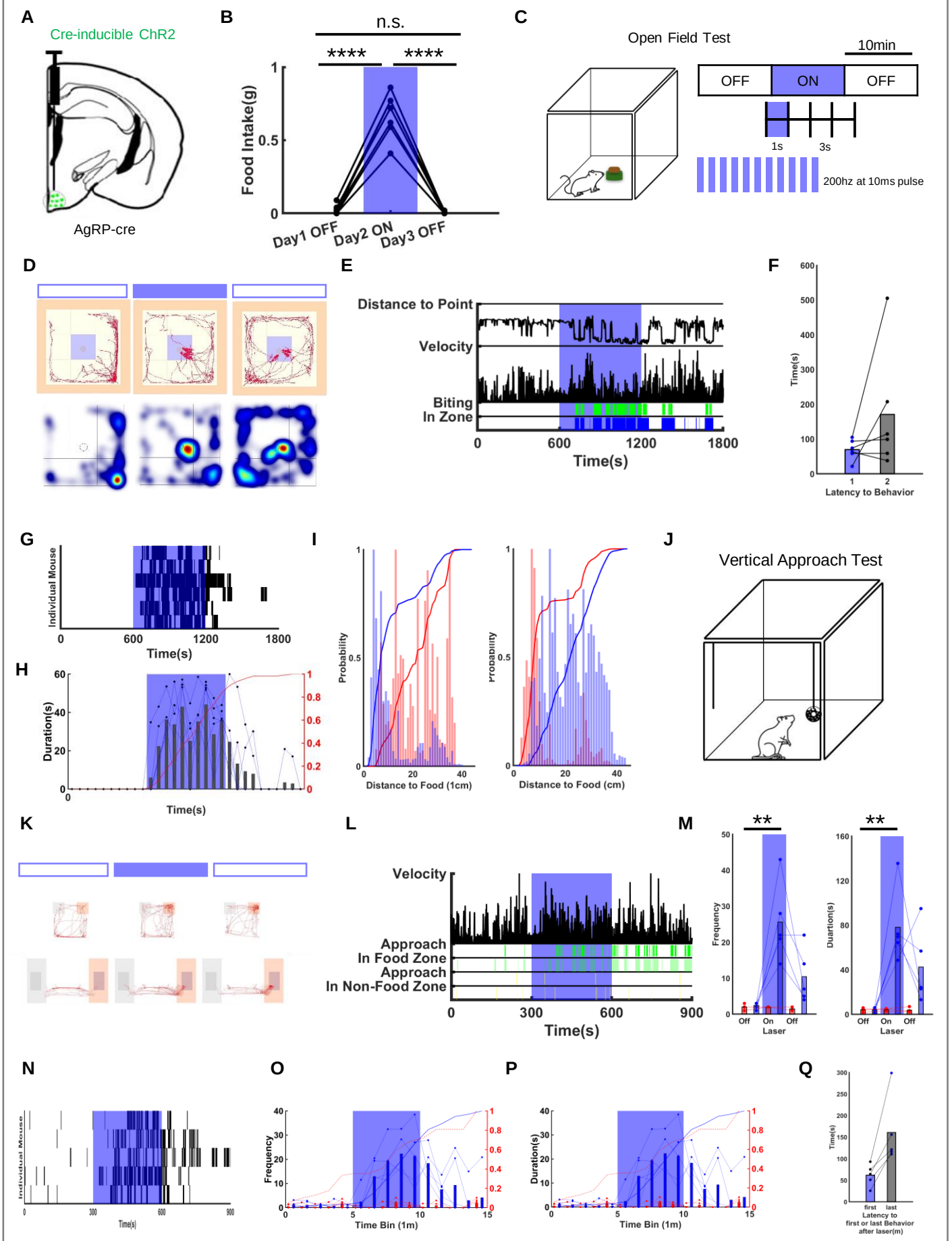
A
Cre-inducible ChR2
AgRP-cre
B
n.s.
****
****
Food Intake(g)
Day1 OFF
Day2 ON
Day3 OFF
C
Open Field Test
10min
OFF
ON
OFF
1s
3s
200hz at 10ms pulse
D
E
Distance to Point
Velocity
Biting
In Zone
Time(s)
F
Time(s)
Latency to Behavior
G
Individual Mouse
Time(s)
H
Duration(s)
Time(s)
I
Probability
Distance to Food (1cm)
Distance to Food (cm)
J
Vertical Approach Test
K
L
Velocity
Approach
In Food Zone
Approach
In Non-Food Zone
Time(s)
M
**
**
Frequency
Duartion(s)
Off
On
Off
Laser
N
Individual Mouse
Time(s)
O
Frequency
Time Bin (1m)
P
Duration(s)
Time Bin (1m)
Q
Time(s)
first
last
Latency to
first or last Behavior
after laser(m)

Figure 4

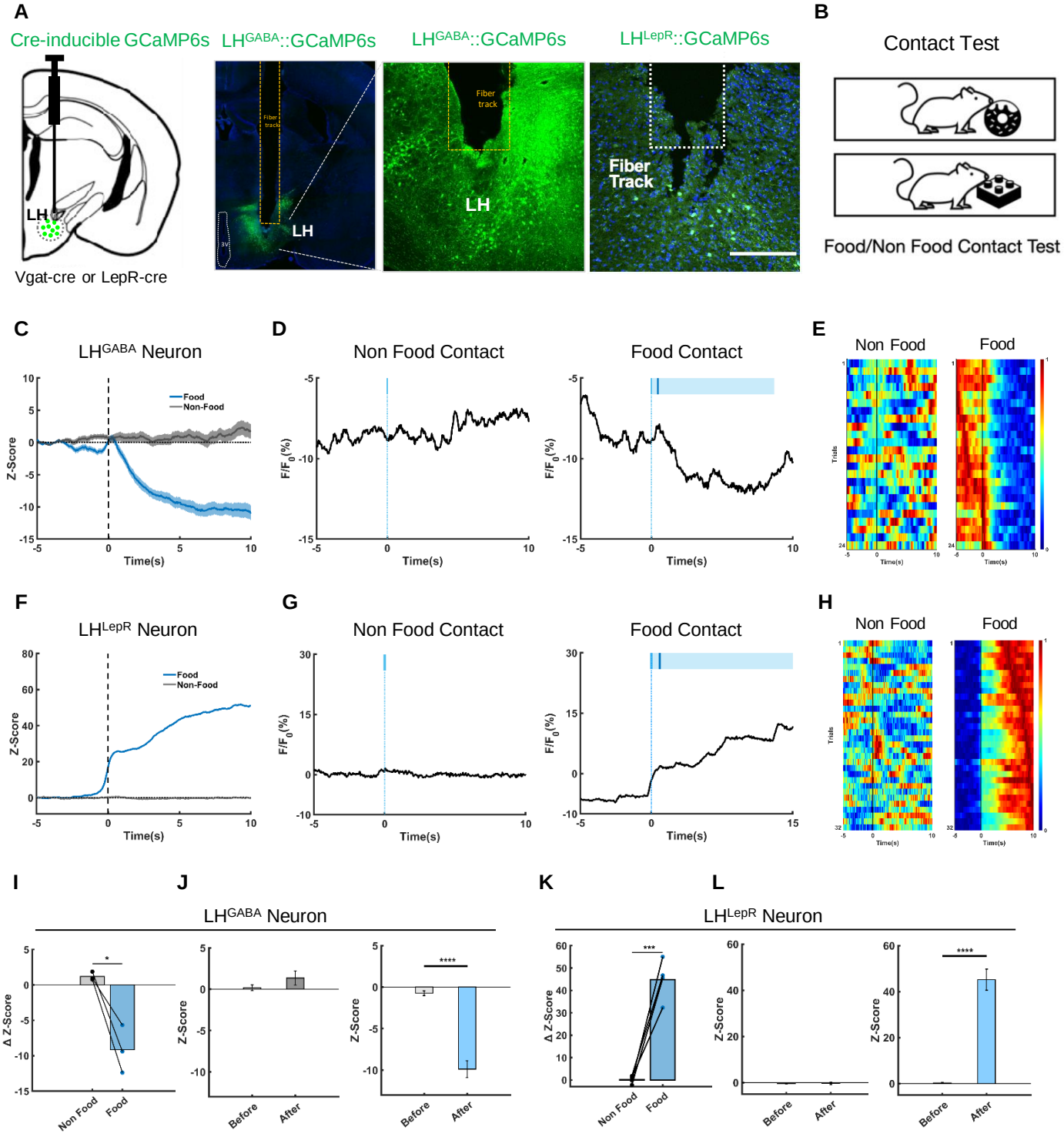
A
Cre-inducible GCaMP6s
LHGABA::GCaMP6s
LHGABA::GCaMP6s
LHLepR::GCaMP6s
LH
Vgat-cre or LepR-cre
Fiber track
LH
Fiber track
LH
Fiber Track
B
Contact Test
Food/Non Food Contact Test
C
LHGABA Neuron
Food
Non-Food
Z-Score
Time(s)
D
Non Food Contact
Food Contact
F/F0(%)
Time(s)
E
Non Food
Food
Trials
Time(s)
F
LHLepR Neuron
Food
Non-Food
Z-Score
Time(s)
G
Non Food Contact
Food Contact
F/F0(%)
Time(s)
H
Non Food
Food
Trials
Time(s)
I
J
LHGABA Neuron
Δ Z-Score
Non Food
Food
Z-Score
Before
After
K
L
LHLepR Neuron
Δ Z-Score
Non Food
Food
Z-Score
Before
After

Figure 5

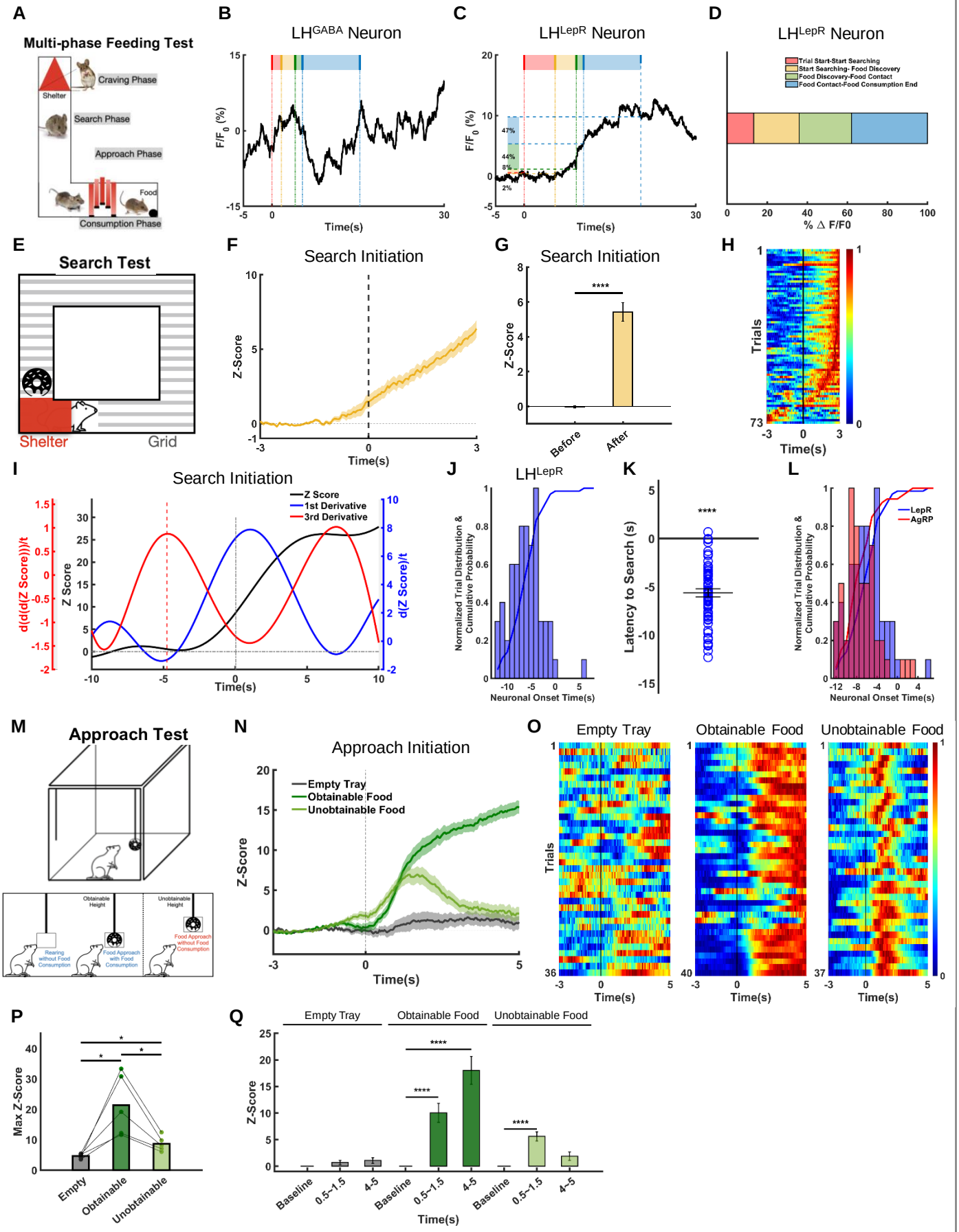
A
Multi-phase Feeding Test
Shelter
Craving Phase
Search Phase
Approach Phase
Food
Consumption Phase
B
LHGABA Neuron
F/F0 (%)
Time(s)
C
LHLepR Neuron
47%
44%
8%
2%
D
LHLepR Neuron
Trial Start-Start Searching
Start Searching- Food Discovery
Food Discovery-Food Contact
Food Contact-Food Consumption End
% Δ F/F0
E
Search Test
Shelter
Grid
F
Search Initiation
Z-Score
G
Search Initiation
****
Before
After
H
Trials
I
Search Initiation
Z Score
1st Derivative
3rd Derivative
d(d(d(Z Score)))/t
d(Z Score)/t
J
LHLepR
Normalized Trial Distribution & Cumulative Probability
Neuronal Onset Time(s)
K
Latency to Search (s)
L
LepR
AgRP
M
Approach Test
Obtainable Height
Unobtainable Height
Rearing without Food Consumption
Food Approach with Food Consumption
Food Approach without Food Consumption
N
Approach Initiation
Empty Tray
Obtainable Food
Unobtainable Food
O
Empty Tray
Obtainable Food
Unobtainable Food
P
Max Z-Score
Empty
Obtainable
Unobtainable
Q
Baseline
0.5~1.5
4~5

Figure 6

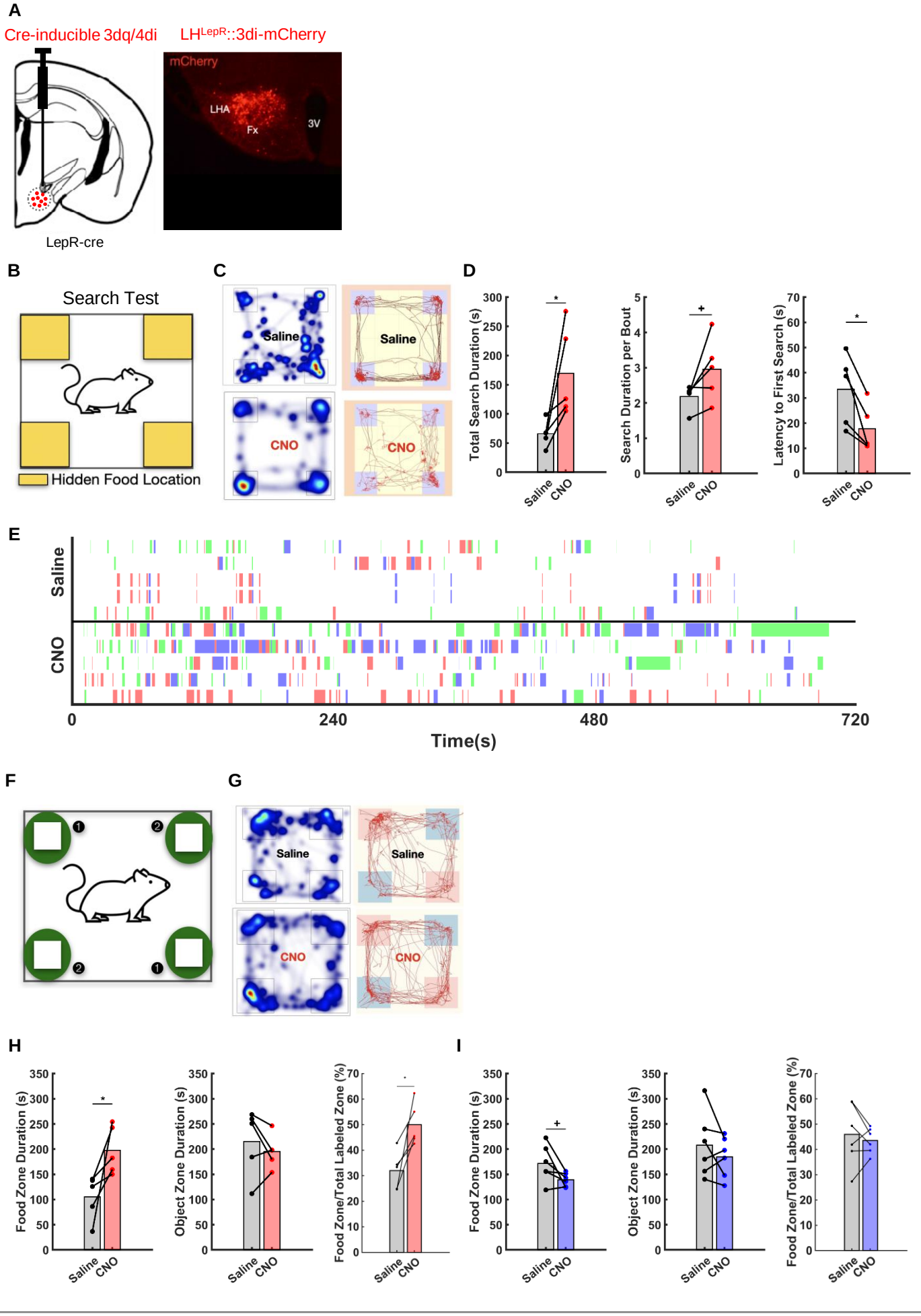
A
Cre-inducible 3dq/4di
LHLepR::3di-mCherry
mCherry
LHA
Fx
3V
LepR-cre
B
Search Test
Hidden Food Location
C
Saline
CNO
D
Total Search Duration (s)
Search Duration per Bout
Latency to First Search (s)
Saline
CNO
E
Saline
CNO
0
240
480
720
Time(s)
F
G
H
Food Zone Duration (s)
Object Zone Duration (s)
Food Zone/Total Labeled Zone (%)
I

Figure 7

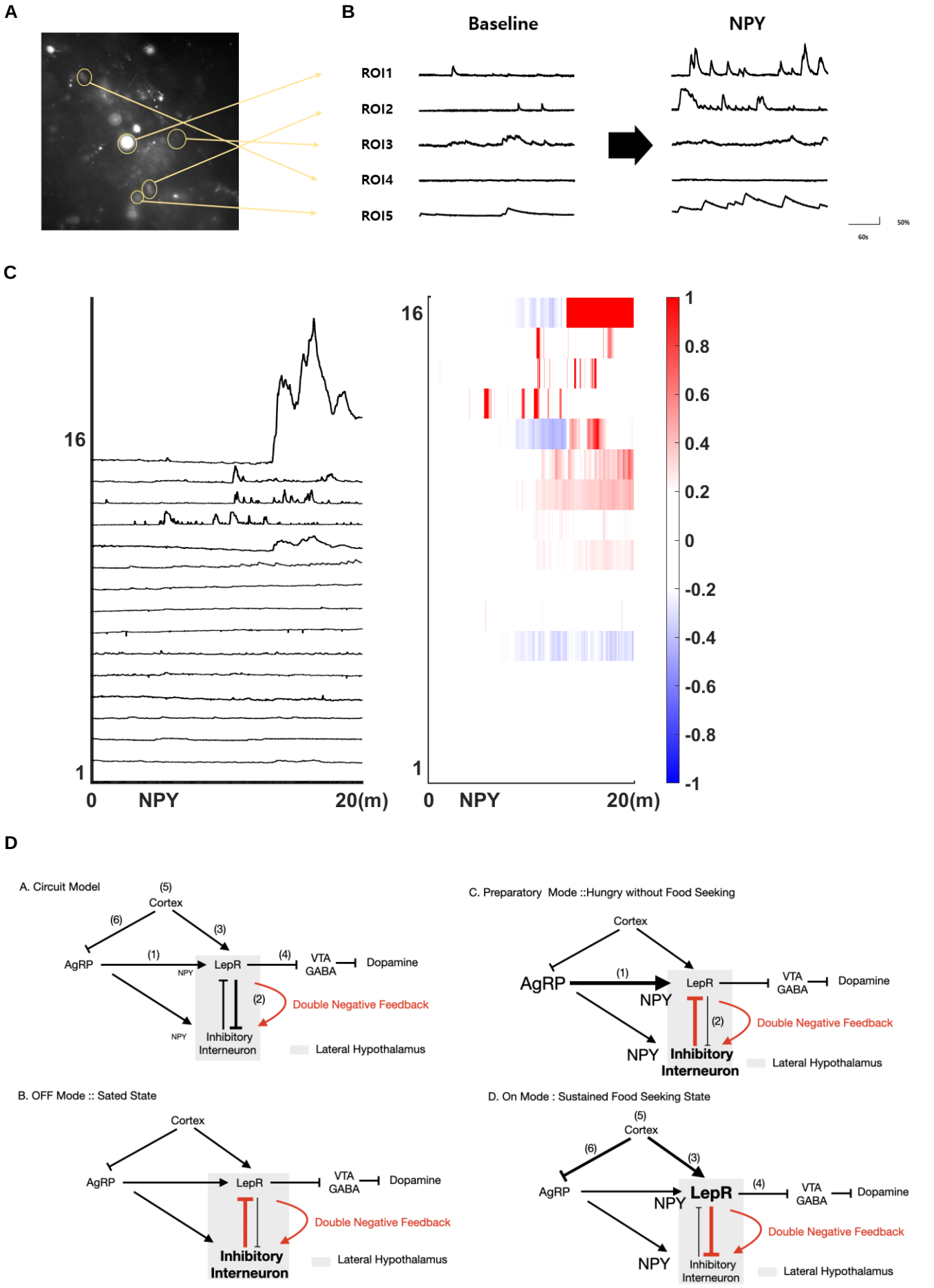
A
B
Baseline
NPY
ROI1
ROI2
ROI3
ROI4
ROI5
50%
60s
C
16
1
0
NPY
20(m)
16
1
0
NPY
20(m)
1
0.8
0.6
0.4
0.2
0
-0.2
-0.4
-0.6
-0.8
-1
D
A. Circuit Model
(5)
Cortex
(6)
(3)
AgRP
(1)
NPY
LepR
(4)
VTA
GABA
Dopamine
(2)
Double Negative Feedback
NPY
Inhibitory
Interneuron
Lateral Hypothalamus
B. OFF Mode :: Sated State
Cortex
AgRP
LepR
VTA
GABA
Dopamine
Double Negative Feedback
Inhibitory
Interneuron
Lateral Hypothalamus
C. Preparatory Mode ::Hungry without Food Seeking
Cortex
AgRP
(1)
LepR
VTA
GABA
Dopamine
NPY
(2)
Double Negative Feedback
NPY
Inhibitory
Interneuron
Lateral Hypothalamus
D. On Mode : Sustained Food Seeking State
(5)
Cortex
(6)
(3)
AgRP
LepR
(4)
VTA
GABA
Dopamine
NPY
Double Negative Feedback
NPY
Inhibitory
Interneuron
Lateral Hypothalamus